ELSEVIER

Tribology International 36 (2003) 255–259

TRIBOLOGY INTERNATIONAL

www.elsevier.com/locate/triboint

Nanoscale friction reduction and fatigue monitoring due to ultrasonic excitation

H. Kutomi [a], A. Daugela [b,*], W.W. Gerberich [c], H. Fujii [a], T.J. Wyrobek [b]

[a] *Mechanical Engineering Department, Gifu University, 1-1 Yanagido, Gifu 501-1193, Japan*
[b] *Hysitron Inc., 5251 West 73rd Street, Minneapolis, MN 55439, USA*
[c] *University of Minnesota, Minneapolis, MN 55455, USA*

Abstract

DLC film interfacial fatigue and changes in friction coefficient phenomena were investigated during quasi-static nanoindentation/scratch while the sample surface was excited ultrasonically. An original experimental setup combines nanoindenter, SPM scanner and ultrasonic transducer operating in an elastic standing wave mode. Nanoindentation loading–unloading curves revealed delamination induced excursions after a certain number of ultrasonic loading cycles. Drastic changes in quasi-statically monitored friction coefficient during nanoscratch were correlated with sample vibration amplitude and loading force. Resulting indentation/scratch film delamination effects and surface wear patterns were examined by an in situ SPM technique. Ultrasonically excited nanoindentation and nanoscratch techniques can be considered as fast and qualitative methods to characterize critical tribo surfaces for data storage devices.

Keywords: Nanoindentation; Nanoscratch; Fatigue; Ultrasonic excitation; Delamination

1. Introduction

Quasi-static nanomechanical testing instruments provide quantitative evaluation of mechanical properties derived at the nanoscale via process of nanoindentation/scratch/wear. Numerous applications include characterization of critical data storage tribo surfaces [1,2]. However, increased operational bandwidth of precise mechanical devices such as hard disk drives (HDD) require study of critical tribo surfaces at ultrasonic frequency ranges. Many scientific efforts have been spent in developing dynamic and ultrasonic techniques, i.e. mechanical-Q monitoring [3,4]. Mechanical properties can be derived at the nanometer scale from mechanical interaction between oscillating nanoindenter tip and an adhering surface [5]. A quartz microbalance technique has been used to derive loss modulus of several nanometer thick polymer films [6]. Friction measurements were introduced in scanning probe microscopy (SPM) measurements by Mate in the early 1990s [7] and since then several attempts have been made to utilize this concept in nanotribology [8]. Friction reduction monitoring is known in micro-scale measurements [9].

Two very fast methods that rely on ultrasonic excitation are introduced for characterization of DLC overcoats for potential HDD applications. DLC film interfacial fatigue and changes in friction coefficient phenomena were investigated during quasi-static nanoindentation/scratch while sample surface was excited ultrasonically. An original experimental setup consists of commercially available quasi-static nanoindentation/scratch instrument interfaced with an SPM and a specially designed ultrasonic transducer, where various modes of standing wave resonance vibrations were generated in the DLC coated silica substrate. Indents and scratches were placed within SPM precision at locations of vibration anti-nodal planes obtained by investigating Chladny patterns. Resulting indentation/scratch wear patterns and film delamination effects were examined by the in situ SPM technique.

* Corresponding author.
E-mail address: daugela@hysitron.com (A. Daugela).

0301-679X/03/$ - see front matter © 2003 Elsevier Science Ltd. All rights reserved.
doi:10.1016/S0301-679X(02)00195-0

2. Fracture mechanics of ultrasonically excited contact

Two theoretical approaches can be considered for deriving relationships between a number of fatigue cycles and mechanical characteristics such as film toughness, elastic modulus and contact geometry [10]. Schematics of reverse-cycling and ratcheting fatigue processes are shown in Fig. 1. The reversed-cycling approach is applicable for rather low number of failure cycles and can be expressed as

$$N_{\mathrm{f}} = \alpha_1\left[\frac{\varepsilon_{\mathrm{f}}}{2\varepsilon_{\alpha}^{\mathrm{P}}}\right]^2, \tag{1}$$

where α_1~1 is an arbitrary constant and ϵ_{f} is the monotonic true fracture strain. Here, the fracture strain is for an elastic-plastic material at or near the contact point. The Manson–Coffin model of ratcheting fatigue can lead to the initial wear damage. The effective fracture strain ϵ_{f} can be expressed in terms of fracture mechanics as follows:

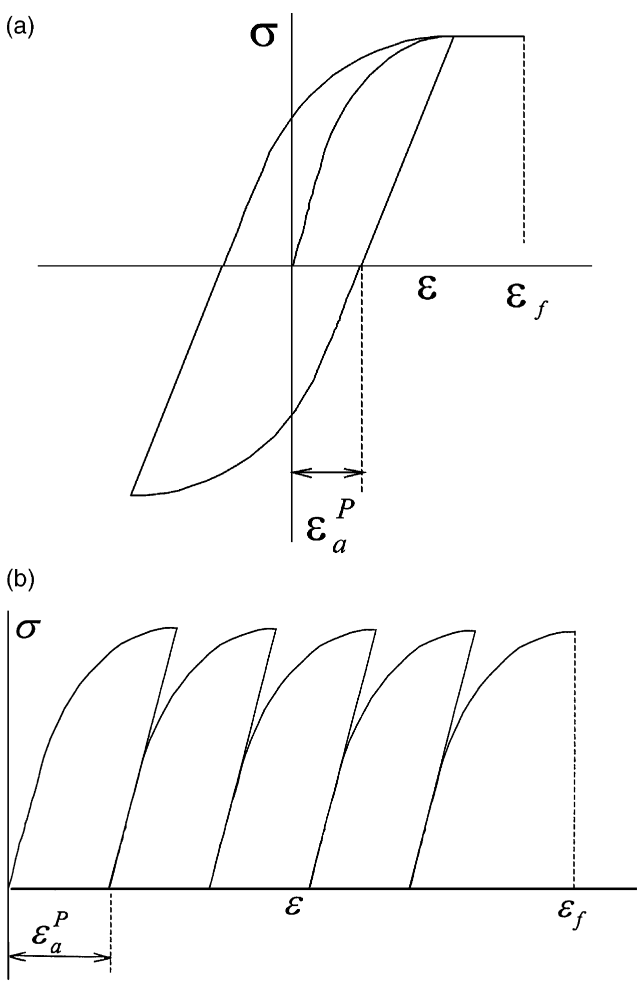

Fig. 1. Micro-fatigue model: (a) reverse-cycling fatigue; (b) ratcheting fatigue.

$$\varepsilon_{\mathrm{f}} = \frac{R_{\mathrm{P}}\sigma_{\mathrm{YS}}}{r \quad E} = \frac{K_{\mathrm{IC}}^2 \quad \sigma_{\mathrm{YS}}}{\pi\sigma_{\mathrm{YS}}^2 r \quad E}, \tag{2}$$

where σ_{ys} is the yield stress and r is the distance from the natural flaw where the fracture strain is exceeded. At the fracture stress of $\varepsilon = \varepsilon_{\mathrm{f}}$, the stress intensity equals the film toughness, $K_{\mathrm{I}} = K_{\mathrm{IC}}$ and E is modulus dominated by the substrate. Following the recent fracture mechanics advances in geometrically necessary dislocations, plastic strain $\varepsilon_a^{\mathrm{p}}$ for a spherical contact can be expressed as

$$\varepsilon_a^{\mathrm{P}} \cong \frac{a}{4R} \cong \frac{\sqrt{2\delta R}}{4R} \cong \left(\frac{\delta}{8R}\right)^{1/2}, \tag{3}$$

where a, R and δ are the contact geometry parameters, i.e. spherical contact radius, radius of the tip and displacement of the tip into the surface, respectively. Thus,

$$N_{\mathrm{f}} \cong \frac{2K_{\mathrm{IC}}^4 R}{\pi^2 r^2 \sigma_{\mathrm{YS}}^2 E^2 \delta}. \tag{4}$$

The only unknown is r, the distance from the natural flaw where the fracture strain is exceeded. We assume this as a fraction, α, of the slip band, l_{s} , piled-up at the film which triggers light wear process induced by an increase in friction. K_{IC} is achieved at r~αl_{s} where film breakthrough occurs at

$$N_{\mathrm{f}} \cong \frac{2K_{\mathrm{IC}}^4 \quad R}{\pi^2 \sigma_{\mathrm{YS}}^2 E^2 (\alpha\lambda_{\mathrm{S}})^2 \delta}. \tag{5}$$

Ratcheting fatigue applied to the single contact would take fewer cycles to produce failure

$$N_{\mathrm{f}} = \alpha_2\left[\frac{\varepsilon_{\mathrm{f}}}{\varepsilon_a^{\mathrm{P}}}\right]. \tag{6}$$

Here, α_2~1 is an arbitrary constant. In this case, the Manson–Coffin fatigue for a single point contact leads to the light wear under ratcheting boundaries which can be expressed by

$$N_{\mathrm{f}} = \frac{K_{\mathrm{IC}}^2}{\pi\alpha\lambda_S\sigma_{\mathrm{YS}}E}\left(\frac{8R}{\delta}\right)^{1/2}. \tag{7}$$

The reverse-cycling and the ratcheting fatigue approaches provide the fundamental basis of understanding and relate fatigue cycle number to the realistic fracture and mechanical parameters. The physical concept of reverse-cycling is that the contact stress magnified by a dislocation pile-up acting on an intrinsic defect in the film and its interface triggers light wear.

An ultrasonically excited nanoscratch on a steel surface can be modeled by the plastic ploughing process induced by a rigid wedge where a combination of shear and normal stress modifies resulting contact pressure. This problem is addressed by Kutomi et al. [11]. Thus, modeling of ultrasonically excited interface brittle to ductile transition during scratch requires more elaborate efforts.

3. Experimental setup and procedures

The experimental setup shown in Fig. 2 consists of the three-capacitance plate quasi-static nanoindentation/scratch tester (Hysitron, Inc.) with in situ SPM imaging option [12]. The noise floors for the lateral and vertical quasi-static displacement and vertical force sensing are 10, 0.1 nm, and 100 nN, respectively. The nanoindentation/scratch tester is interfaced with a SPM (AFM) scanner (Digital Instruments Co.). A nanoindentation/scratch tester is attached to the SPM scanner. An originally designed ultrasonic transducer is placed on the SPM scanner. It consists of a piezo element attached to the bottom of a DLC sample-waveguide and an acoustic isolator. An ultrasonic transducer is driven at one of the resonance standing modes by a wave generator. Frequency response characteristics of waveguide and one of the Chladny patterns are shown in Fig. 3, where elastic compression wavefront gradients are plotted schematically. A DLC film coated silica sample is placed on the anti-nodal plane of waveguide vibration at location ‘a’. Selected grain sand (~5 μm) was used for visualization of Chladny patterns. The ultrasonic transducer was driven at the resonance mode by a wave generator at a frequency of 207 kHz. The nanoscratch/nanoindentation tester and the SPM scanner were controlled by two dedicated data acquisition systems. A SPM scanner was used for in situ imaging of post-indents/scratches. An SPM type Berkovich diamond tip with the radius of 100 nm was used as an indentation and scratching tool. Maximum sample vibration amplitude of 6 nm was found by means of independent LDV measurements. The DLC film was 100nm thick with a 20nm interlayer of Ni between the DLC and the silica substrate.

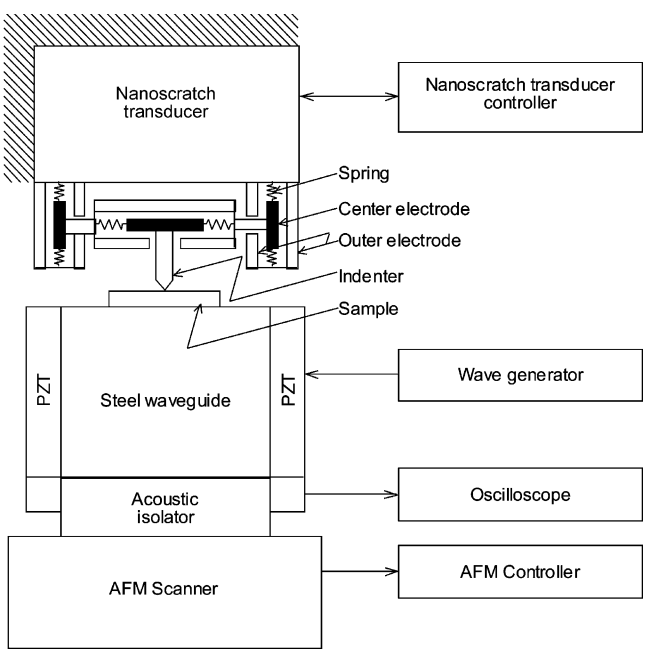

Fig. 2. Experimental setup.

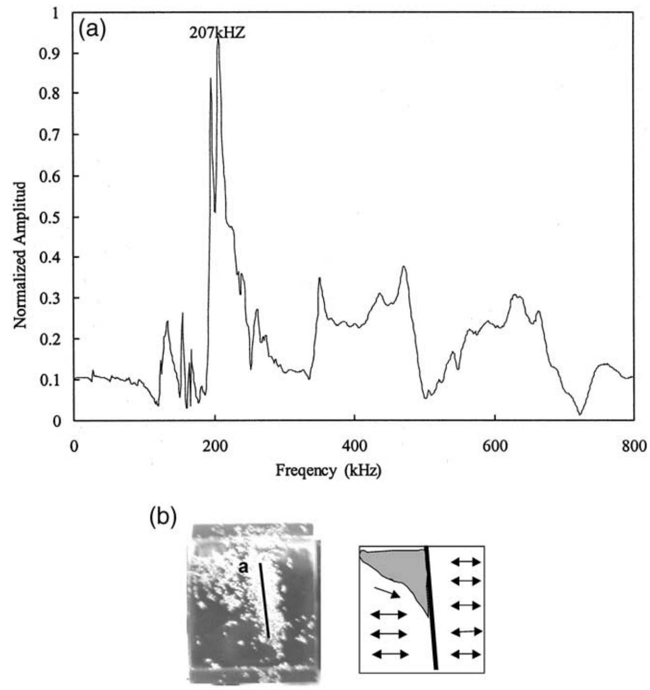

Fig. 3. (a) Frequency response of waveguide; (b) visualized Chladny pattern of waveguide surface.

4. Experimental results

4.1. Ultrasonically excited nanoindentation

Nanoindentation loading–unloading curves for ultrasonically excited and non-excited DLC film sample are shown in Fig. 4 for the normal loading force of 3000

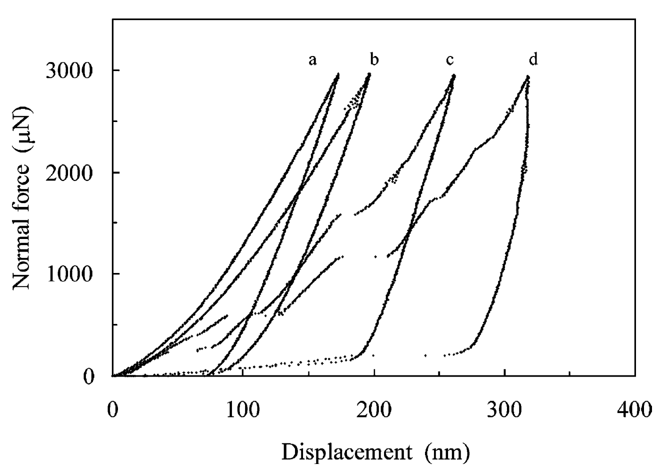

Fig. 4. Nanoindentation loading–unloading curves.

μN. Here, case ‘a’ corresponds to the ultrasonically not excited indentation. The cases ‘b’, ‘c’ and ‘d’ correspond to the ultrasonically excited indentations carried out at normalized amplitudes of 0.25, 0.5 and 0.75 sample vibration maximum amplitude, respectively. Quasi-static ramp loading and unloading processes carried on for 12 s generated over 1,200,000 dynamic nanometer scale loading cycles. Loading segments for curves ‘c’ and ‘d’ indicated well-expressed excursions that resulted in film delamination as it was verified by post-indentation SPM type scans shown in Fig. 5. Elevation of delaminated film can be observed by investigating unloading segments that are dominated by an excessive force. Reduced Young’s modulus and hardness values derived from ‘a’ and ‘b’ unloading curves by the classical nanoindentation approach were 127 and 38 GPa, respectively. Differences in modulus and hardness values for both indentation curves were within 3% indicating that nanoindentation test alone cannot uncover fatigue induced material changes. Careful investigation of ‘b’, ‘c’ and ‘d’ loading–unloading curves revealed changes that can be associated with the dynamics of the film delamination process.

4.2. Ultrasonically excited nanoscratch

Friction coefficient was investigated as a function of quasi-static scratch loading force and arbitrary ultrasonic vibration amplitude. A 20-nm DLC film sample with $R_a = 4$ nm roughness was excited in elastic standing mode at 207 kHz. Quasi-static normal load nanoscratches of 50, 100, 150, 200, 250 μN ramped at 5 s were placed on the sample vibration anti-nodes. Fig. 6 summarizes result derived from approximately 300 nanoscratches of 5 μm length each. Here, a friction coefficient taken as a ratio of lateral and normal forces is

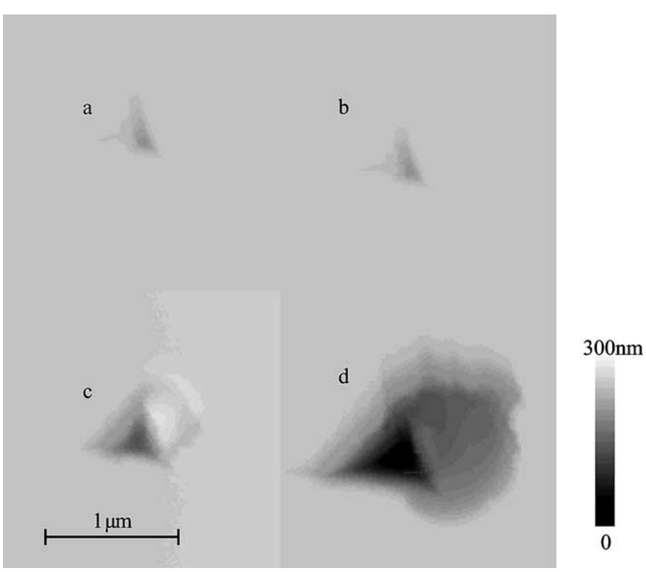

Fig. 5. SPM image of nanoindents.

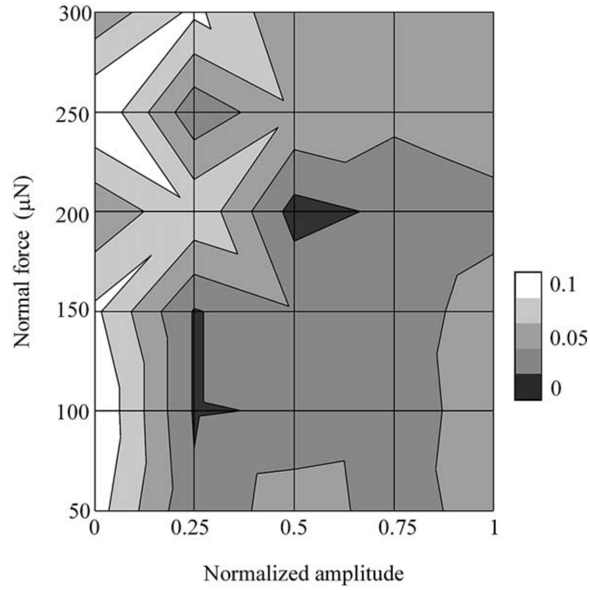

Fig. 6. Friction coefficient as a function of quasi-static normal force and normalized vibration amplitudes of the sample.

plotted as a function of normal load and normalized sample vibration amplitudes. Zones of reduced and increased friction coefficient can be differentiated clearly on the map. An absolute value of friction coefficient was reduced from 0.15 to 0.05 due to the ultrasonic excitation. An SPM type post-scratch scan and corresponding cross-sections are shown in Fig. 7. Here, position ‘a’ corresponds to the case with no ultrasonic excitation. Positions ‘b’, ‘c’, ‘d’ and ‘e’ correspond to the cases of ultrasonic excitation at normalized amplitudes of 0.175, 0.25, 0.5 sample vibration maximum amplitude, respectively. Post-scratch SPM images revealed larger amount of material removed by the larger ultrasonic vibration amplitudes for the cases ‘d’ and ‘e’, where DLC chipping and delamination effects were found. The case ‘b’ indicates the lowest friction coefficient on the friction coefficient map in Fig. 3, where the smallest amount of material was removed from the sample.

It should be noted that friction coefficient measurement on DLC film in ambient environment without ultrasonic excitation did not always yield to repeatable data. In contrast, ultrasonically excited friction coefficient measurements were very consistent. As it was mentioned already, a combination of shear and normal stresses modifies contact pressure under the scratch tool, changes lateral force and affects quasi-statically determined friction coefficient.

5. Conclusions

Two innovative experimental methods are introduced for characterization of DLC type overcoat films. These methods are based on the ultrasonically excited

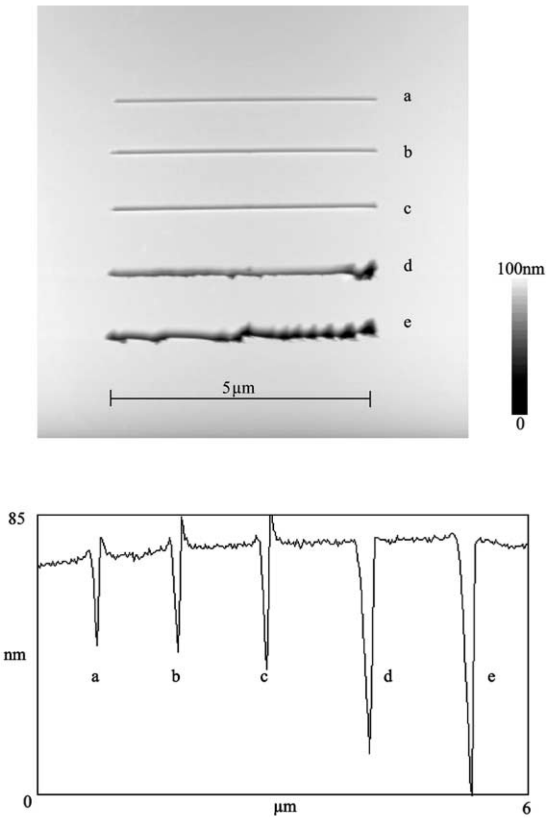

Fig. 7. SPM image of nanoscratches.

nanoindentation/scratch and can provide a very fast wear/fatigue test at the local contact. A quasi-static nanoindentation/scratch instrument interfaced with a SPM and specially designed ultrasonic transducer were used, where various modes of standing wave resonance vibrations were generated in the DLC coated silica substrate. Indents and scratches were placed within SPM precision at locations of vibration anti-nodal planes obtained by investigating of Chladny patterns.

An ultrasonically excited indentation induced DLC film interface fatigue and delamination, which was observed on the loading–unloading curve excursions and verified by post-indentation in situ SPM imaging. A number of cycles and a sample vibration amplitude are two variation parameters in order to find a critical number of interface fatigue cycles producing film interface delamination. Ultrasonically induced interface fatigue can be described by ratcheting and reverse-cycling fatigue models. It should be pointed out that further theoretical development is needed for the Manson–Coffin and the Kapoor–Johnson fatigue approaches in order to have an appropriate analytical prediction tool covering multicycle ultrasonic excitation.

An ultrasonically excited nanoscratch test revealed changes in friction coefficient. A quasi-statically monitored 20% reduction in friction coefficient was observed at rather small excitation amplitudes. Increase in sample oscillation amplitudes yields drastic (up to 40%) increase in friction coefficient induced ultrasonically. Post-scratch in situ SPM type images correlated friction coefficient changes with ultrasonically induced wear marks and film chipping. Film chipping indicated a transition of ductile to brittle interface. Qualitative friction coefficient maps can be developed by means of multiparameter fitting routines to characterize unknown DLC based tribo surfaces.

Ultrasonically induced nanoindentation/scratch measurements are sought as fast qualitative/quantitative techniques for overcoat films.

References

[1] Li X, Bhushan B. Micro/nanomechanical and tribological characterization of ultrathin amorphous carbon coatings. J Mater Res 1999;14(6):2328–37.
[2] Tan S, Prabakaran V, Talke FE. Investigation of nano and micro wear of magnetic tape head materials. Tribol Int 2000;33:673–81.
[3] Kazushi K, Maruyama Y, Tsuji T. Resonance frequency and Q factor mapping by ultrasonic atomic force microscopy. Appl Phys Lett 2001;78(13):1939–41.
[4] Rabe U, Amelio S, Kopycinska M, Hirsekorn S, Göken M, Arnold W. Imaging and measurement of local mechanical material properties by atomic force accoustic microscopy; 2001.
[5] Syed Asif SA, Wahl KJ, Colton RJ. Rev Sci Inst 1999;70:2408.
[6] Krim J, Dayo A, Daly C. In: Cohen SH, Lightbody ML, editors. Atomic force microscopy/scanning tunneling microscopy. New York: Plenum Press; 1994. p. 21-1.
[7] Mate CM, McClelland GM, Erlandsson R, Chiang S. Phys Rev Lett 1987;59:1942.
[8] Carpick RW, Ogletree DF, Salmeron M. Lateral stiffness: a new nanomechanical measurement for the determination of shear strengths with friction force microscopy. Appl Phys Lett 1997;70(12):1548.
[9] Kutomi H, Sase N, Fujii H. Development of friction controller. Proc Int Conf AMPT'99 1999;1:605–12.
[10] Gerberich WW, Tymiak NI, Kramer DE, Daugela A. An approach to dry friction and wear for small volumes. Philos Mag, in press.
[11] Kutomi H, Daugela A, Fujii H, Wyrobek TJ. Wear, in press.
[12] Bhushan B, Kulkarni AV, Bonin W, Wyrobek JT. Philos Mag 1996;A74(5):1117–23.